

Influence of the thickness and area of NiCr/Ag electrodes on the characteristics of BaTiO₃- ceramic based positive-temperature-coefficient thermistors

B. HEINEN, R. WASER

Institut für Werkstoffe der Elektrotechnik, Rheinisch–Westfälische Technische Hochschule Aachen, 52056 Aachen, Germany
E-mail: waser@iwe.rwth-aachen.de

The electrical behaviour of commercial BaTiO₃-based positive-temperature-coefficient (PTC) thermistors with NiCr/Ag electrodes was investigated by impedance analysis in the frequency domain. The contact resistance and thus the total resistance of the PTC increases with decreasing thickness as well as with decreasing area of the NiCr layer at constant Ag top layer. The increase in the total resistance in both cases is explained by the increase in the contact area of the Ag layer to the ceramic which is represented by a model. The Ag forms a blocking contact to the ceramic in contrast to the NiCr which shows an ohmic behaviour. Using our model, the electrode impedance contribution of very thin NiCr layers can be interpreted in terms of incomplete wetting of the ceramic surface by the NiCr metal during the deposition. Supplementary scanning electron microscopy and high-resolution transmission electron microscopy analyses have been used to study the structure of the electrode interface and the structure of the layers. © 1998 Kluwer Academic Publishers

1. Introduction

Barium-titanate-based positive-temperature-coefficient (PTC) thermistors are used in a variety of applications, including current limiting, temperature sensing, degaussing and protection against overheating in equipment such as electric motors. They are also employed in level indicators, in time delay devices, in thermostats and as compensation resistors. Semiconducting n-doped barium titanate exhibits an increase in resistance of several orders of magnitude in the vicinity of the Curie temperature [1]. Electrode contacts to semiconducting oxides with ohmic characteristics are required to exploit the conductivity–temperature range of the ceramic to its full extent. In industrial applications, NiCr/Ag electrodes commonly are formed by combining a NiCr layer and a Ag top layer. NiCr serves as an ohmic contact and provides good adhesion to the ceramic while Ag prevents corrosion and guarantees good solderability and ensures uniformity of electric field across the PTC.

At present the ohmic behaviour of InGa electrodes as well as NiCr/Ag electrodes is well known [2–7] in contrast with, for example, pure Ag electrodes which form a blocking contact to the PTC ceramic [3, 6, 7, 8].

However, the correlation between the role of NiCr as an adhesive layer and as an ohmic contact for the PTC components is not known yet. In the present paper, this aspect will be analysed by investigation of the as yet insufficiently known influence of the thickness of the NiCr layer on the resistance. Likewise, the contact area of the NiCr layer should influence the total resistance of the thermistor at constant area of

the top layer. With the aid of modern analytical methods the electrode interface can be investigated systematically.

In the present paper, we represent analytical scanning electron microscopy (SEM) investigations of a cross-section of the ceramic–electrode system, which have been performed to obtain information about the formation of the interface and the thickness of the NiCr and the Ag layer. The morphological contact between the ceramics and the NiCr layers has been investigated by high-resolution transmission electron microscopy. These analyses should show the crystal structure of the ceramic, the structure of the NiCr layer at the ceramic interface and at the NiCr–Ag interface, and the crystal structure of the Ag layer.

The microstructure of ceramics can be simplified by a brick wall model and can be represented by an electrical network consisting of three RC branches due to the bulk of the grains, the grain boundary regions and the electrical interfaces [9, 10]. From the measurement of the complex impedance, the electrode interface resistance can be calculated as well as the grain and the grain-boundary resistance [2–4].

As reference electrodes, NiCr/Ag electrodes and InGa electrodes were applied and investigated since they exhibit completely ohmic characteristics. The contact behaviour of Ag electrodes which form a blocking contact has been studied, too. In order to study the influence of the combination of the NiCr layer and the Ag top layer, the thickness and the area of the NiCr layer were altered with a constant Ag layer. A model was introduced to explain the influence

of these modifications on the contact resistances. Additional finite-element method (FEM) simulations should support this model.

2. Experimental procedure

Commercial PTC ceramics without electrodes were obtained from Philips Components Industrial. The PTC ceramic was BaTiO_3 based and in the form of dense discs with a diameter of 10 mm and a thickness, $d = 2.7$ mm.

The NiCr/Ag electrodes (thickness, 100–200 nm) and the Ag electrodes (thickness, 200 nm) were deposited by thermal evaporation on both sides of the ceramic with a diameter of 9 mm. In order to study the influence of the combination of NiCr and Ag electrodes the thickness of the NiCr layer was altered (10, 30 and 100 nm) at a constant thickness of the Ag layer (200 nm). Likewise, the area of the NiCr layer was varied (diameters, 3, 5 and 7 mm) at a constant area of the Ag layer (diameter, 9 mm). The InGa electrodes as reference electrodes with completely ohmic contacts were applied by a simple rubbing method (diameter, 10 mm). SEM (Zeiss DSM 982 Gemini) investigations were performed on a cross-section of the ceramic with NiCr (100 nm)/Ag (3 μm). HRTEM (JEOL 4000 EX) studies were done at the interfaces between the BaTiO_3 ceramic and NiCr layer and between the NiCr layer and the Ag layer.

The impedance measurement were conducted at room temperature using a Hewlett–Packard LF 4192A impedance analyser with a frequency range from 5 Hz to 12.6 MHz. As usual, the microstructure of ceramics is considered to be sketched in the three-dimensional cross-section and simplified by a brick wall model as shown in Fig. 1 [9]. The model illustrates the polarization and the conduction contributions to the total impedance of the system which can be represented by an electrical network consisting of three RC branches. Four RC branches would be necessary for measurements in the time domain because of the non-linear behaviour of the cathode/ceramic/anode system. This plays an important part in, for example, SrTiO_3 thin films [11]. Owing to a small-signal excitation for investigations in the frequency domain the equivalent circuit consisting of a single parallel RC branch combining anode and cathode impedances can be used in this model for BaTiO_3 ceramics. The elements of the network may be attributed to the permittivities, conductivities and geometrical extensions of the bulk of the grains (indicated by subscript b), the grain boundaries (indicated by subscript gb), and the electrode interfaces (indicated by subscript el).

The total impedance of this model is given by the equation

$$Z_{\text{tot}} = Z_{\text{el}} + Z_{\text{b}} + Z_{\text{gb}} = \text{Re}(Z) - i \text{Im}(Z) \quad (1)$$

where $\text{Re}(Z)$ and $\text{Im}(Z)$ are the real part and the imaginary part, respectively.

The plot of the imaginary part of the total impedance against the real part (the so-called Cole–Cole plot) delivers three independent semicircular arcs as shown in Fig. 2. The highest-frequency arc

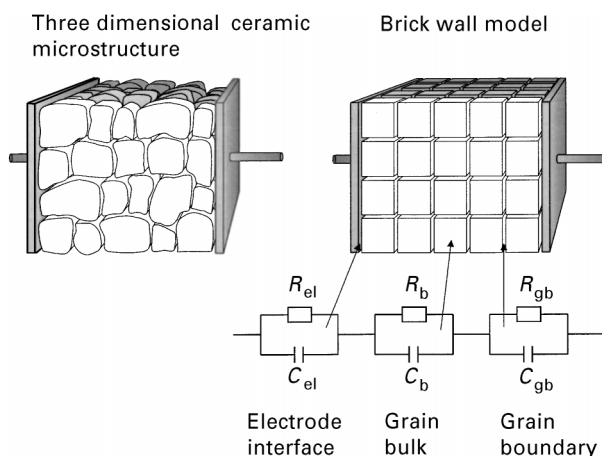


Figure 1 Sketched three-dimensional cross-section of a ceramic with applied electrodes, the corresponding simplified brick wall model and the electrical equivalent network.

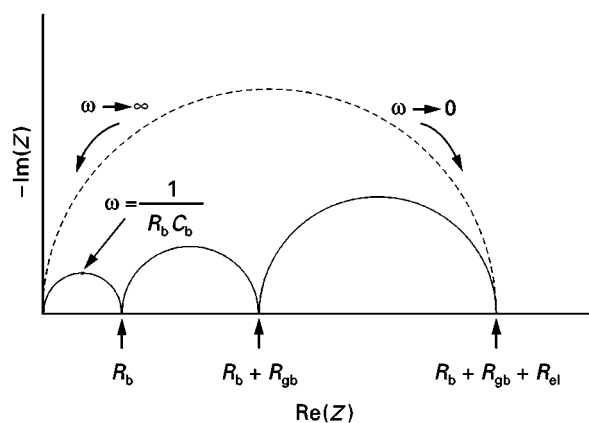


Figure 2 Idealized impedance plot, the so-called Cole–Cole plot, for measurements in the frequency domain of a ceramic consisting of grains and grain boundaries with electrodes.

corresponds to the bulk conduction, the intermediate frequency arc to the grain-boundary conduction, and the lowest-frequency arc to the electrode interface process. The resistance values of the circuit elements are obtained from the real-axis intercept while the capacitance values are obtained from the frequency corresponding to the highest point in each semicircle. Thus, the contact resistance, R_{el} , can be separated from the measured impedance of the sample in a low-frequency region.

A non-ideal behaviour of the semicircular arcs can be observed in case of practical tests which has been shown as depressed arcs, a melding of the arcs, and displacements of the arcs from the real axis [3, 12, 13, 14].

3. Results and discussion

3.1. Scanning electron microscopy–high-resolution transmission electron microscopy analysis.

The analytical investigation of a cross-section of a ceramic with NiCr/Ag electrodes by SEM studies is shown in Fig. 3. The thicknesses of the NiCr layer and

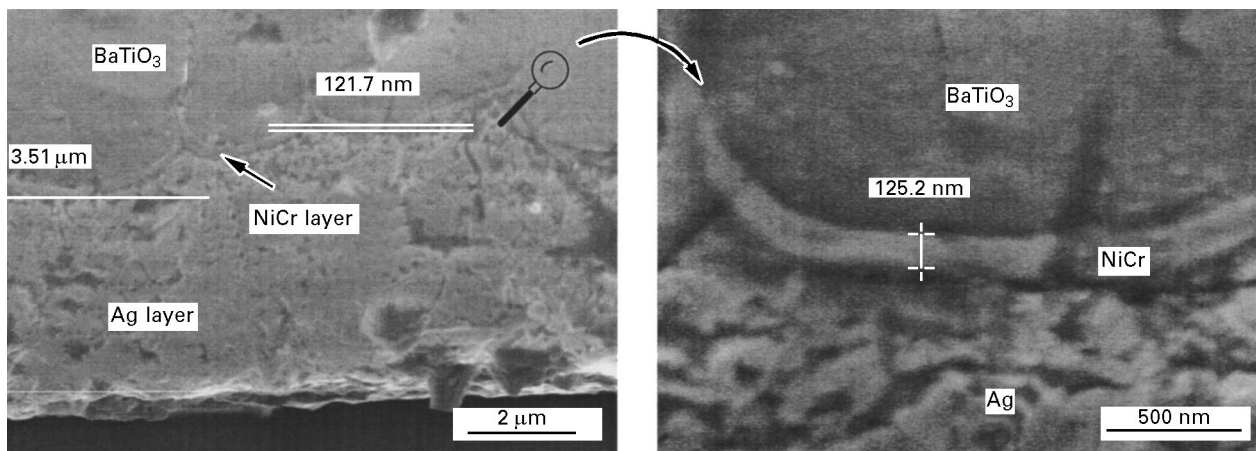


Figure 3 Scanning electron micrographs of a cross-section of BaTiO₃-based ceramic with a NiCr/Ag electrode.

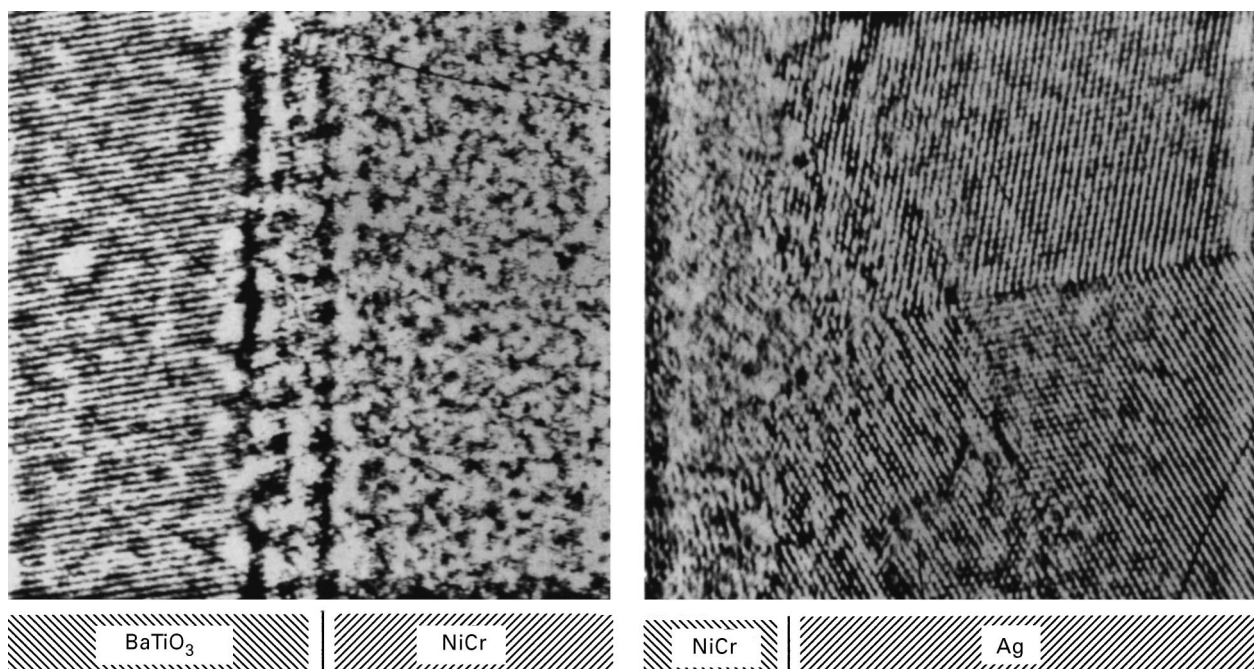


Figure 4 High resolution transmission electron micrographs of the interfaces between a BaTiO₃-based ceramic and a NiCr layer and between the NiCr and Ag layers.

the Ag layer are from this analysis approximately 120 nm and approximately 3.5 μm, respectively. Likewise, the cross-section reveals the very high roughness of the ceramic surface. It is also noted from this figure that the NiCr wets the ceramic surface completely.

Fig. 4 illustrates the analysis of the same cross-section by HRTEM studies. This analytical study reveals more information about the contact of the ceramic and the layers and about the layers themselves. The crystalline crystal structure of the ceramic and of the silver layer can be clearly seen. Likewise, Fig. 4 shows the amorphous crystal structure of the NiCr layer and the interface to the ceramic. This means that the NiCr could not crystallize at the cold sample in the evaporation process owing to the high melting point of the alloy NiCr ($T_m \approx 1400^\circ\text{C}$). The NiCr layer at the NiCr–Ag interface seems to be crystalline. This could be explained by alloying of the NiCr layer and the Ag layer.

3.2. Effect of the electrode material

In order to gain insight into the ceramic–electrode interface, the sample with three different electrode materials was studied by impedance analysis. Fig. 5 shows the Cole–Cole plots for a sample with InGa electrodes and NiCr/Ag electrodes as examples of ohmic contacts. Only one semicircular arc was obtained corresponding to the grain boundaries. Because of the limited frequency region, the arc due to the bulk of the grains could not be observed. The resistance of the bulk can be calculated as $R_b = 5\Omega$ and the resistance and capacitance values of the grain boundaries are $R_{gb} = 22\Omega$ and $C_{gb} = 2.9\text{ nF}$, respectively.

For non-ohmic Ag electrodes on a PTC BaTiO₃ ceramic, the impedance data were similar to those for the InGa and NiCr/Ag electrodes with the addition of a second arc at low frequencies as shown in Fig. 6. This arc is indicative of a blocking contact (Schottky barrier) at the electrode–ceramic interface. The

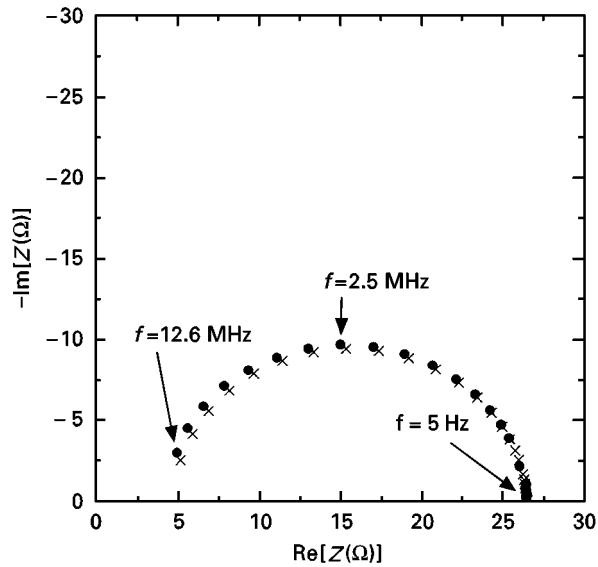


Figure 5 Impedance plots of BaTiO₃-based ceramics with InGa (●) and NiCr/Ag (×) electrodes at room temperature.

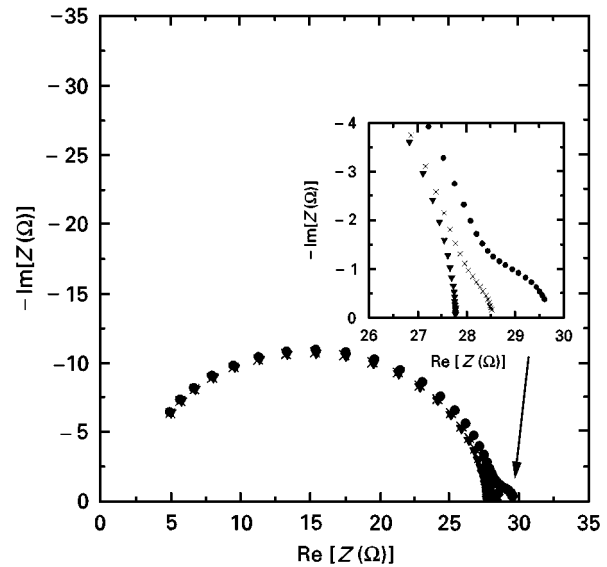


Figure 7 Impedance plots of a BaTiO₃-based ceramics with NiCr/Ag electrodes, where the thickness of the NiCr layer was altered at constant thickness of the Ag top layer of 200 nm at room temperature. (●), 10 nm NiCr; (×), 30 nm NiCr; (▼), 100 nm NiCr.

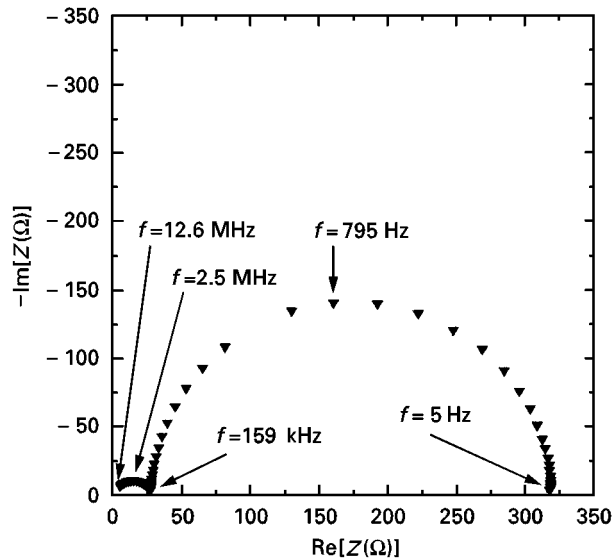


Figure 6 Impedance plot of a BaTiO₃-based ceramic with Ag (▼) electrodes at room temperature.

interface resistance and capacitance can be calculated as approximately $R_{e1} = 300\Omega$ and approximately $C_{e1} = 6.5\text{ nF}$, respectively, which is in good accordance with previous work [3, 7]. Several experimental data, however, show a large scatter in the resistance value where the standard deviation is about 10% of the mean value. This large scatter has already been found for Au electrodes, for example [4, 7, 11].

Vollmann and Waser [9] neglected the influence of the two electrode interfaces because of the large number of grain boundaries crossing the current path between the electrodes. This assumption is acceptable for SrTiO₃ ceramics owing to its high ohmic character but the electrode influence has to be taken in consideration for BaTiO₃ ceramics [2–4] as well as for SrTiO₃ single crystals [10]. Dietz *et al.* [11] found in their investigations for SrTiO₃ thin films that the overall film resistance has to be regarded as primarily determined by the electrode–film interface depending on the type of the metal but not on the bulk of the thin film in comparison with this work.

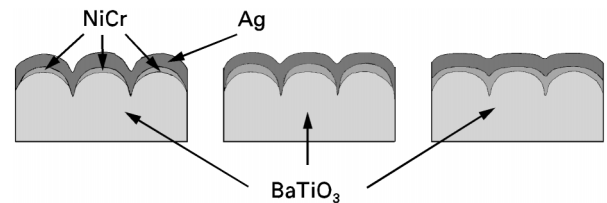


Figure 8 Sketched model of the ceramic with a NiCr/Ag electrode with altered NiCr layer thickness.

3.3. Effect of the NiCr layer thickness

The thickness of the adhesion layer plays an important part for PTC applications which is shown in Fig. 7. A small increase in the electrode resistance with decreasing NiCr layer thickness at constant thickness of the Ag top layer is shown. Thus, it is important to have at least 100 nm thick a NiCr layer for good ohmic contact between the ceramic and the electrodes.

The simplified model in Fig. 8 presents an explanation of the measured results. If a thin layer of NiCr was applied on the very rough surface of the ceramic, island formation would be expected. In particular, the metal layer does not coat the deep grain boundaries completely. Therefore, a blocking contact between the Ag layer and the ceramic occurs in the grain-boundary regions, which is representative in the Cole–Cole plot. With increasing layer thickness of the NiCr layer up to 100 nm the area of direct contact between the Ag and the BaTiO₃ vanishes and the influence of the non-ohmic contact at the Ag–ceramic interface disappears.

In order to check this hypothesis, model electrodes of different NiCr areas underneath a constant Ag top layer should be prepared and investigated.

3.4. Effect of the NiCr layer area

Fig. 9 shows the strong increase in the total resistance with decreasing area of the NiCr layer at a constant

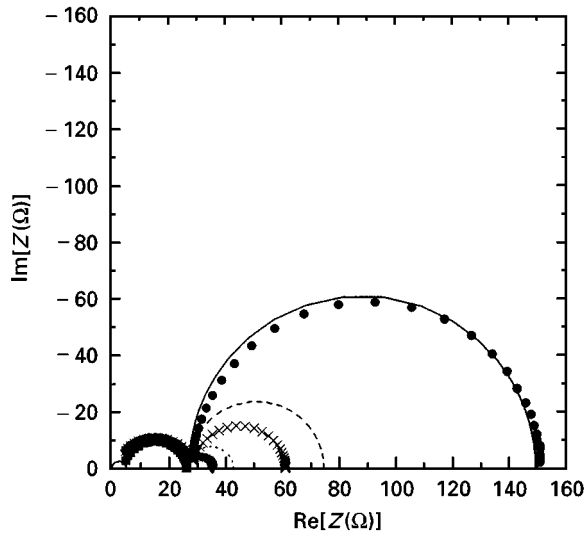


Figure 9 Impedance plots of a BaTiO₃-based ceramics with NiCr/Ag electrodes (●), (×), (▼), (■) experimental data; (—), (---), (····), (— · — ·), calculations), where the area of the NiCr layer was altered at constant area of the Ag top layer (diameter, 9 mm) at room temperature. (●), (—), diameter of 3 mm; (×), (---), diameter of 5 mm; (▼), (····), diameter of 7 mm; (■), diameter of 9 mm.

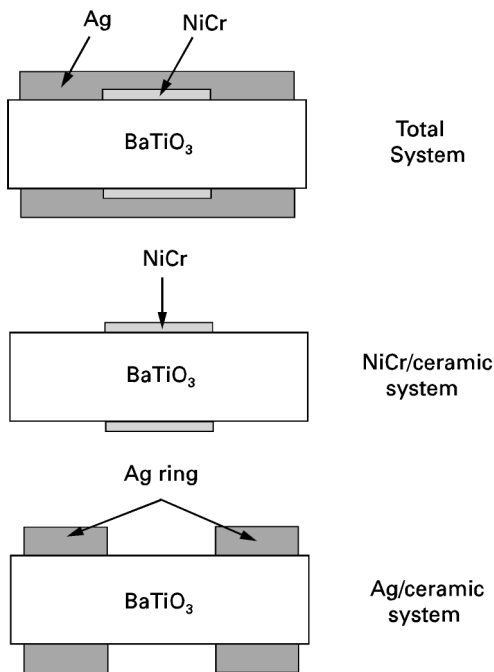


Figure 10 Sketched models of the total ceramic/NiCr/Ag electrode system, the NiCr/ceramic system and the Ag/ceramic system.

area of the Ag layer (diameter, 9 mm). The growth of the influence of the electrode interface is determined by the increasing contact area of the Ag and the BaTiO₃.

Thus, the ceramic/NiCr/Ag system can be considered as a combination of two systems as shown in Fig. 10. The NiCr/ceramic system is representative of an ohmic contact while the Ag/ceramic system constitutes a blocking contact. Consequently the total impedance, Z_{tot} , of the ceramic/NiCr/Ag system can be calculated from a parallel connection of the

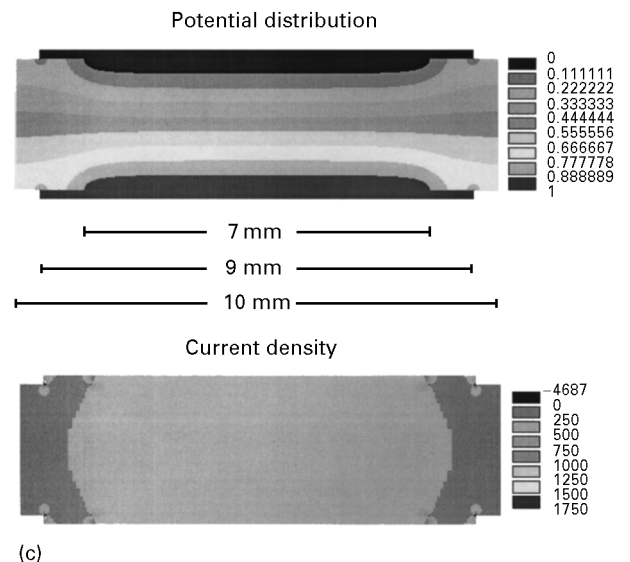
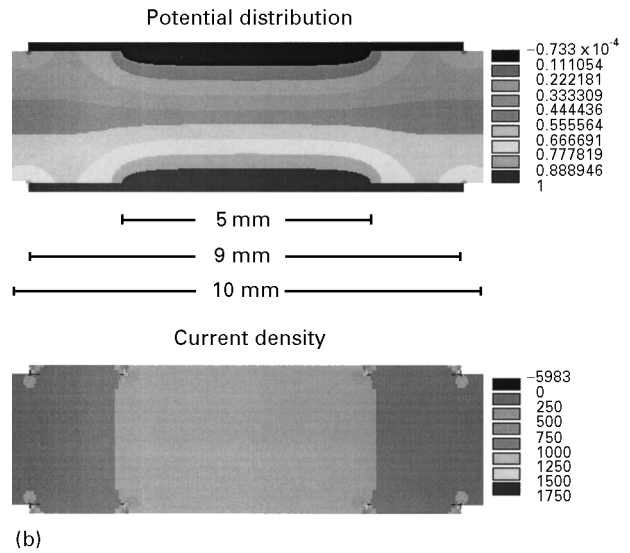
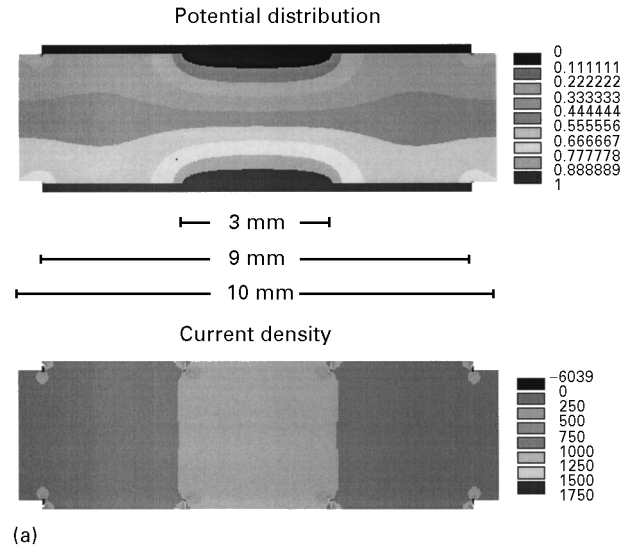


Figure 11 Potential contribution and current density of a ceramic with a NiCr layer and a corresponding Ag ring layer simulated by the FEM for various diameters of the NiCr layer: (a) 3 mm; (b) 5 mm; (c) 7 mm.

impedances of the ceramic/NiCr and the ceramic/Ag systems which can be written as

$$Z_{tot} = \frac{Z_{NiCr} Z_{Ag}}{Z_{NiCr} + Z_{Ag}} \quad (2)$$

The impedance of the metal–metal interface NiCr–Ag can be neglected. The calculated impedance values can be taken from the measurements of the ceramic with NiCr electrodes shown in Fig. 5 and from the measurements of the ceramic with Ag electrodes shown in Fig. 6 by consideration of the geometrical extensions of the bulk, the grain boundaries and the electrodes. The calculated total impedances which were obtained from Equation 2 are shown in Fig. 9 and represent the also shown experimental impedance values of the complete system ceramic/NiCr/Ag to a first approximation. The deviations in the calculated values from the measured impedances increase with increasing NiCr area.

To quantify this finding, the total impedance of the ceramic/NiCr/Ag system was simulated by FEM (ANSYS). Fig. 11 show the potential distributions and current densities of the ceramics with NiCr/Ag electrodes with NiCr diameters of 3 mm (Fig. 11a), 5 mm (Fig. 11b) and 7 mm (Fig. 11c) and additionally the corresponding Ag ring areas. In order to simulate the blocking contact between the Ag ring and the ceramic a high ohmic interface layer inside the ceramic with contact to the ceramic was assumed. These simulations reveal an increase in the deviation of the effective area to the expected area of the current density with increasing NiCr area. These deviations correspond well to the differences between the calculated and experimental impedance values shown in Fig. 9. This means that the model which is shown in Fig. 10 is an excellent explanation for the measured effects.

With the help of Equation 2 it is now possible to calculate the effective contact area between the Ag layers and the ceramics in the case of the vanishing NiCr thickness in Section 3.3. The effective Ag contact area was estimated as 2.2% for a NiCr layer 30 nm thick and as 4.5% for a NiCr layer 10 nm thick.

4. Conclusions

In this paper we report the effect of thickness and area variations of the ohmic NiCr contact layer of NiCr/Ag electrodes on BaTiO₃-based PTC thermistor ceramics.

Below a critical thickness of the NiCr layer, a significant contribution of the electrode to the total

impedance appears. This contribution increases with a further reduction in the NiCr layer thickness. Since a morphologically perfect contact between the BaTiO₃ ceramics and the NiCr layer was detected by HRTEM analysis, we attributed this additional impedance contribution to incomplete wetting of thin NiCr layers and, hence, a reduction in the effective area of the ohmic contact. In order to check this hypothesis, model electrodes of different NiCr areas underneath a constant Ag top layer were prepared. Impedance spectroscopy data and additional FEM simulations strongly supported the incomplete wetting model.

Acknowledgements

The authors would like to thank Philips Components Industrial for the supply of PTC samples, the support and helpful discussions. The HRTEM studies performed by Dr Jia of the Forschungszentrum Jülich are gratefully acknowledged.

References

1. W. HEYWANG, *Solid-State Electron.* **3** (1961) 51.
2. H. S. MAITI and R. N. BASU, *Mater. Res. Bull.* **21** (1986) 1107.
3. D. P. CANN and C. A. RANDALL, *J. Appl. Phys.* **80** (1996) 1628.
4. S.-O. YOON, H.-J. JUNG and K.-H. YOON, *Solid State Commun.* **64** (1987) 617.
5. J. NARAYAN and V. N. SHUKLA, *J. Appl. Phys.* **51** (1980) 3444.
6. A. DEGUIN, P. MORETTI and J. P. BOYEAUX, *Ferroelectrics* **26** (1980) 761.
7. M. A. A. ISSA, *Mater. Sci.* **27** (1992) 3685.
8. Z. SUROWIAK, J. DUDEK and YU. I. GOLTZOV, S. G. GACH, A. P. DRANISHNIKOV, L. A. SHPAK, V. E. YURKEVICH, *Ferroelectrics* **123** (1991) 19.
9. M. VOLLMANN, R. WASER, *J. Amer. Ceram. Soc.* **77** (1994) 235.
10. R. WASER, M. KLEE, *Integrated Ferroelectrics* **2** (1992) 23.
11. G. W. DIETZ, W. ANTPÖHLER, M. KLEE and R. WASER, *J. Appl. Phys.* **78** (1995) 6113.
12. J. R. MACDONALD, *J. Chem. Phys.* **61** (1974) 3977.
13. J. E. BAUERLE, *J. Phys. Chem. Solids* **30** (1969) 2657.
14. A. D. FRANKLIN, *J. Amer. Ceram. Soc.* **58** (1975) 465.

Received 11 July 1997

and accepted 2 April 1998